Delta J. Sci. 2008, 32: 1 -31

GEOLOGY

# Petrogenesis of Gabal El Kahfa Ring Complex, Eastern Desert of Egypt.

**Wifky S. A. El-Naggar**

*Nuclear Materials Authority, P.O. Box: 530 El-Maadi, Cairo, Egypt*

*(Received: 15 Oct. 2008)*

**Abstract:** Gabal El Kahfa ring complex occurs in the southern Eastern Desert, Egypt, at the intersection of lat. 24o 8/ 18// N and long. 34o 38/ 55// E on the northern side of Wadi El Khrit . The ring complex exhibits incomplete type forming a horse-shoe ridge opened to the south, where the central stock (~ 1 km in diameter) is located near the southern openning.

Petrographically the diorite and porphyrites (Metavolcanic) represent the country rocks of the area. The ring complex is represented by alkali syenites and quartz syenites in the outer ring and the melanocratic synenites. Also the central stocks are mainly represented by essexite gabbros and different dykes. The studied syenitic rocks are characterized by the presence of perthitic feldspar and plagioclase feldspar which mean that they are subsolvus.

The geochemical features revealed that the syenitic rocks of Gabal El Kahfa ring complex originated from metaluminous alkaline magmas that developed in within plate tectonic setting being generated at depth of about 9-21 km equivalent to 3-6 kb and temperature more than 840°c with multi-processes of both assimilation and fractional crystallization involving plagioclases, hornblende and Fe-Ti oxides from a partial melted lithospheric magma.

The total rare earth elements (REE) concentrations show an increase from the outer ring to the inner ring and have positive correlation with silica content which indicates that there are separate magmatic pulses. The chondrite-normalized REE patterns of the studied samples of the inner and outer ring complex show strong light rare-earth element (LREE) enrichment over the heavy rare-earth elements (HREE) displaying pronounced fractionation and the negative Eu anomaly and consistent with plagioclase fractionation. The REE composition of the outer ring structure was achieved at 49% fractional crystallization whereas that the inner ring structure was achieved at 53% crystal fractionation.

The relations between U and Th elements reflects enrichment with magmatic differentiation. Also, the behavior of U and Th respect to Rb show there is thus a close link between Rb, Th and U in the evolution of magmatic series whether this evolution follows magmatic processes. It is clear that the U and Th contents are controlled by the presence of some accessory minerals (zircon, allanite, apatite and iron oxides) whereas iron oxide and hydroxides have the ability of adsorbing uranium from circulating solutions.

## Introduction

Following the progressive cratonization of the late Proterozoic intra-oceanic island-arcs systems, post-orogenic granites of Pan-African age were emplaced throughout the Arabian-Nubian Shield (ANS), (Almond,1979; Stoeser and Elloit, 1980, Vail, 1984). Two lithologic associations have been recognized, viz, the Younger Granite association and the Syenite association.

The syenite association particularly occurs in the Arabian sector of (ANS), in southeast Egypt and northeast Sudan as ring-complexes confined to narrow bands trending ENE or NNW, which appear to be related to brittle fracturing of the cratonized basement subsequent to the end of the tectonic events (e.g.El Ramly et al. 1971; Vail, 1984, 1985). Mostly, these complexes are made up of alkali granites, quartz syenites, trachytes and gabbros. They form prominent peaks and geologically much younger ranging in age from 540-88 Ma (Hashad and El-Reedy, 1979; Serencsists et al., (1979; 1981); 440-88 Ma Stern and Hedge, (1985).

Vail (1989) distinguished the ring complexes into two major groups according to their tectonic settings during their emplacement: (a) Plate –margin environment of oceanic crust characterized by island arcs and subduction related magmatism and adjacent continental margin where magmatism ranges from calc-alkaline to alkaline; late-, to post-orogenic intrusive complexes belong to this stage of orogenesis, (b) Within-plate anorogenic magmatism occurs within the continent, and is best exemplified by the Phanerozoic complexes post-dating the Pan-African orogeny.

Based on local morphological and structural criteria, El Ramly et al. (1971) classified the syenite association in Egypt into the following groups: a) Complete ring complexes, b) Incomplete ring complexes, c) Plugs, domes and ring dikes, d) Isometric masses. Each group has its characteristic lithology and sequence of emplacement.

Meneisy (1990) reviewed the geochronalogical studies on the ring complexes in the Eastern Desert, Egypt. He placed El Kahfa ring complex in the Late Cretaceous- Early Tertiary volcanic phase (90±20Ma). The ages reported for El Kahfa ring complex range from a Rb/ Sr isochron age of 81.4 Ma (Hashad and El Reedy, 1979). Also, Serencsits et al. (1979; 1981) reported a series of K/Ar ages on separated biotites ranging from 96 to 88 Ma.

The aim of this study is to describe the mineralogical and chemical characteristics of the El Kahfa ring complex,in order to recognize the magma source, the sequence of magmatic differentiation, and the tectonic setting in which the complex evolved.

## Geologic Setting

Gabal El Kahfa ring complex occurs in the southern Eastern Desert, Egypt at the intersection of lat. 24o 8/ 18// N and long. 34o 38/ 55// E on the northern

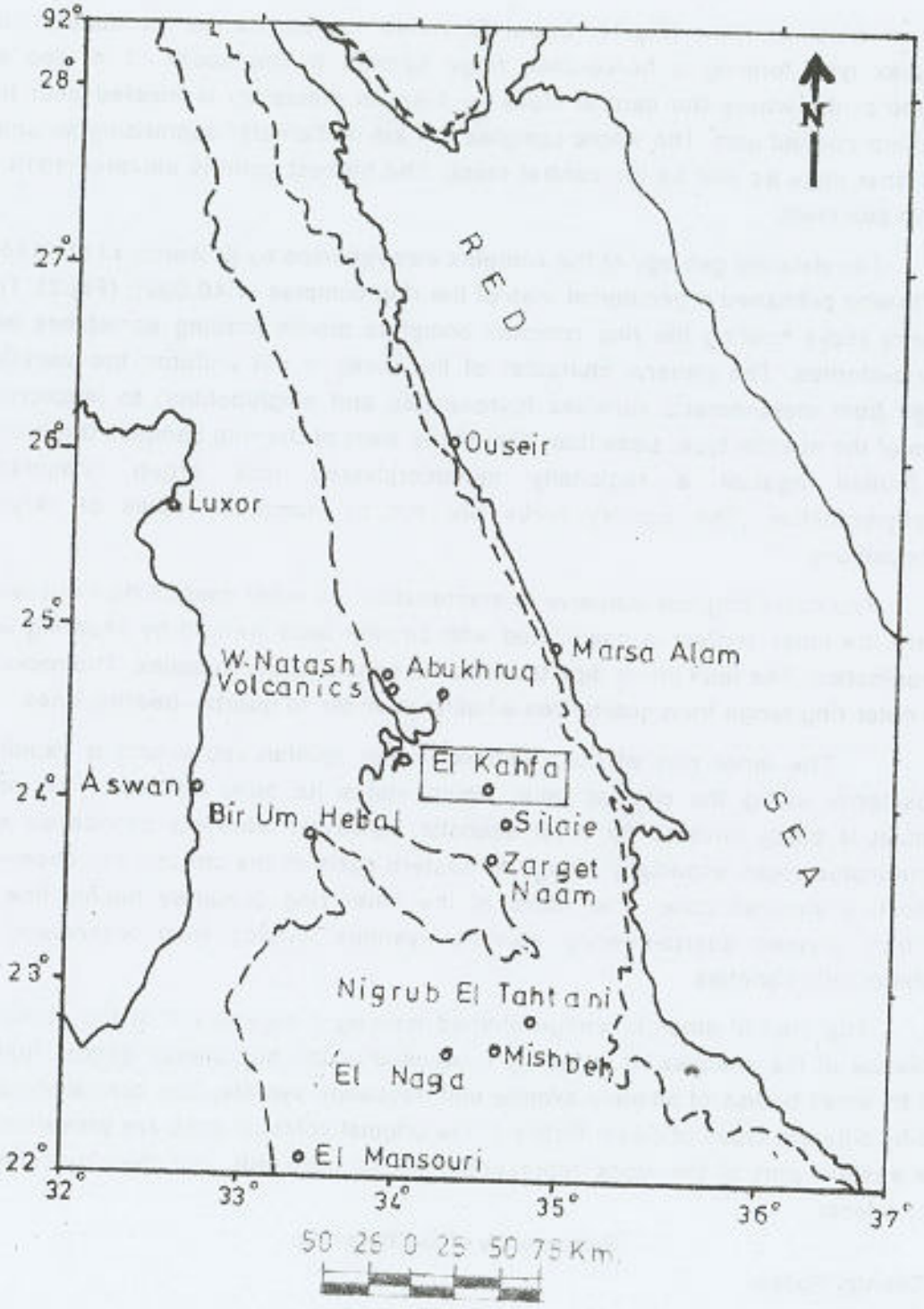


Fig. (1): Distribution map of the Ring Complexes in Eastern Desert. The studied ring complex is in the box.

side of Wadi El Khrit (Fig.1). Gabal El Kahfa represents an incomplete ring complex type forming a horse-shoe ridge opened to the south. It is also an eccentric ring where the central stock (~ 1 km in diameter) is located near the southern opened part. The whole complex is 4 km in diameter comprising an outer and inner rings as well as the central stock. The highest point is elevated 1018 m above sea level.

The detailed geology of the complex was reported by El Ramly et al. (1969; 1971) who published a geological map of the ring complex (1:40,000). (Fig.2). The country rocks hosting the ring complex comprise diorite grading sometimes into quartz-diorites. The general character of the rocks is not uniform; the varieties range from melanocratic varieties (pyroxenites and amphibolites) to leucocratic ones of the syenite type. Less than 1km to the west of the ring complex the diorite is faulted against a regionally metamorphosed rock group comprising porphyroblastics. The country rocks are cut by numerous dikes of varying compositions.

The outer ring has intrusive characteristics; its outer contact dips outwards where the inner contact is associated with circular fault marked by shearing and ferrugination. The fault plane dips towards the central of the complex. The rocks of the outer ring range from quartz-free alkaline syenites to quartz –bearing ones.

The inner ring of the complex, in my opinion represents a cauldron subsidence along the circular fault, which marks its outer contact. The inner contact is partly covered by Wadi deposits, however, intensely cataclased and ferruginated rocks especially along the eastern parts of the contact are observed indicating sheared zone. The rocks of the inner ring comprise mainly fine to medium grained quartz-bearing alkaline syenites varying from leucocratic to melanocratic varieties.

The central stock is wedge shaped forming a conical hill at the southern entrance of the complex. It is mostly composed of the hornblende gabbro that is cut by small bodies of alkaline syenite and nepheline syenite. The central stock is cut by different types of dikes. Relics of the original volcanic cone are preserved in the eastern part of the stock represented by trachybasalts and their pyroclastic equivalents.

## Petrography of El Khafa ring

### A-Country Rocks

### 1- Diorites.

The diorites are grey coloured, massive and inequigranular rocks. They are composed of plagioclase, mafic minerals, quartz and opaques. Microscopically they show a hypidomorphic texture and composed essentially of plagioclase, hornblende, biotite and relics of augite, rounded grains of quartz and opaques. The accessories are apatite, sphene and zircon (Fig: 3-a, b&c).

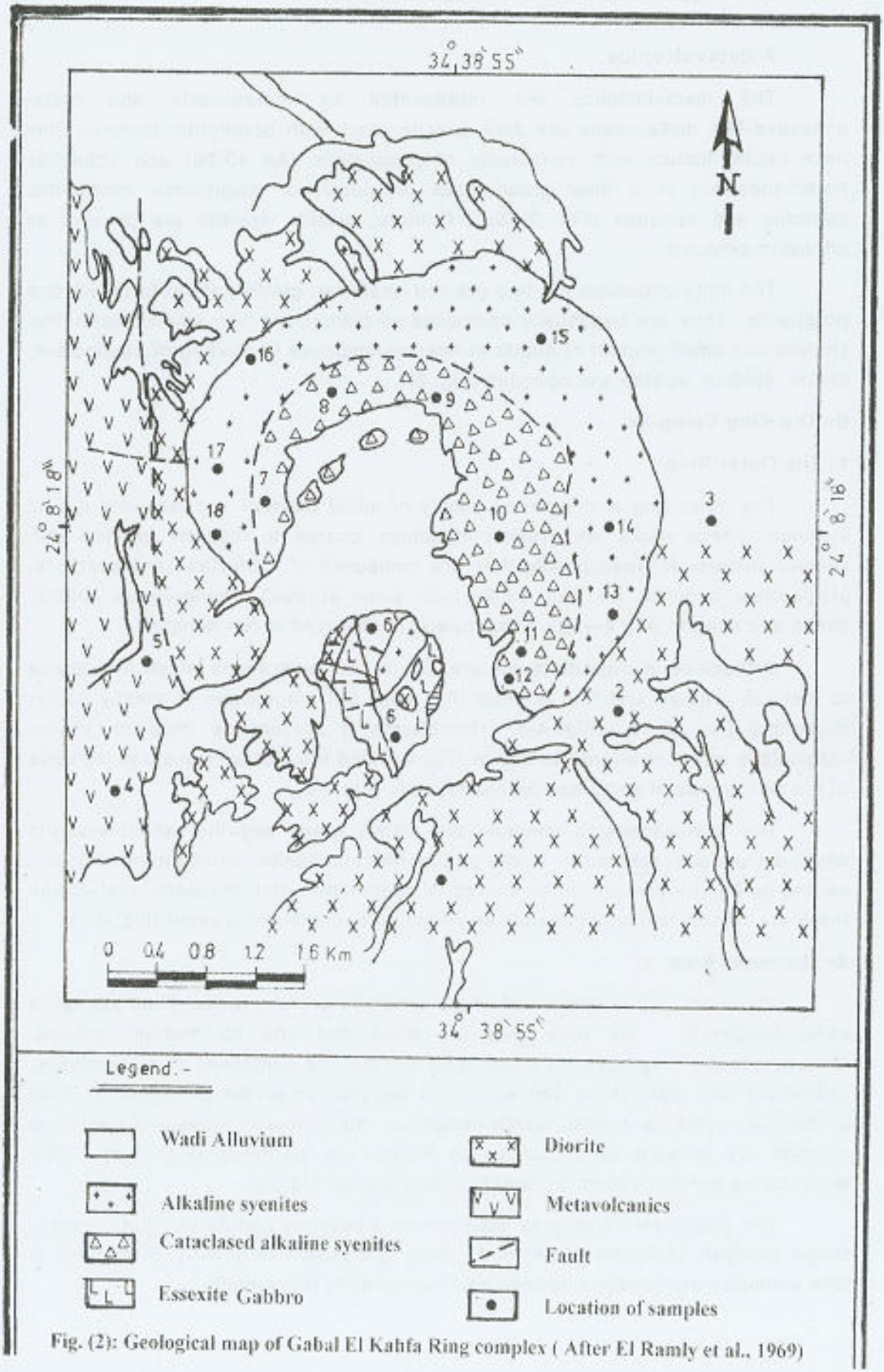


Fig. (2): Geological map of Gabal El Kahfa Ring complex ( After El Ramly et al., 1969)

**2-Metavolcanics.**

The metavolcanics are represented by metabasalts and meta-andesites.The metabasalts are dark grey to black with porphyritic texture. They have fluidal texture with xenoblasts of plagioclase (An 45-50) and actinolitic hornblende set in a finer groundmass composed of plagioclase microlaths, tremolite and opaques (Fig: 3-d&e). Chlorite, zoisite, epidote are present as alteration products.

The meta-andesites are fine grained, massive, greyish green in colour and porphyritic .They are essentially composed of plagioclase (An 40-45), actinolite, chlorite and small amount of quartz in finer groundmass consisting of plagioclase, biotite, epidote, apatite and opaques (Fig: 3f).

**B- The Ring Complex**

**1- The Outer Ring**

The outer ring is composed mainly of alkali feldspar syenites and quartz syenites. These rocks are greyish in colour, coarse to medium grained with syenitic texture. Microscopically they are composed of orthoclase microperthite, plagioclase, aegerine and iron oxides with some accessory minerals as apatite, zircon and sphene (Fig 4-a, b). Some quartz is observed in few samples.

Orthoclase microperthite are present in two generations which are coarse to medium grained and fine grained (Fig 4-a). But plagioclase is mostly albite-oligoclase (An 10-18) (Fig 4-d). Hornblende is present as inclusion in the plagioclase and it is altered to biotite (Fig 4-f) and the biotite inclusions increase at the peripheries of some hornblende crystals (Fig 4-b).

The ferromagnesian minerals are mainly green aegirine, aegirine-augite which are usually replaced by biotite and titaniferous augite. Small amont of quartz as fine grains are present in the interstitial spaces between feldspars crystals and there are some accessory minerals as zircon and apatite are present (Fig: 4- c).

**2- The Inner Ring**

The inner ring is composed of melanocratic syenitic rocks. They appear in hand specimen as dark grey in colour and fine to medium grained. Microscopically, they have hypidiomorphic texture and composed of plagioclases, orthoclase and titaniferous aguites. Some samples show the presence of small amount of nepheline crystals which occure as prismatic and elongated nepheline crystals are present as inclusions in biotite and perthites (Fig: 5-a). The accessories are dominated by apatite minerals (Fig: 5-a, b).

The plagioclase feldspars have pericline twinning and its anorthite content range between 45-58(An 45-58) and zoning is common (Fig: 4-e). Orthoclase is less abundant and always untwined and has perthitic intergrowth.

(a) Microphotograph showing Plagioclase, hornblende and quartz in diorite. C.N. X=10

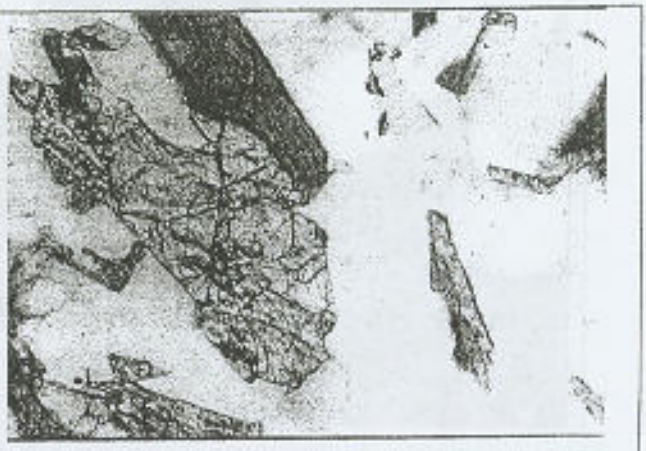

(b) Microphotograph showing augite and biotite in diorite. P.L. X=20

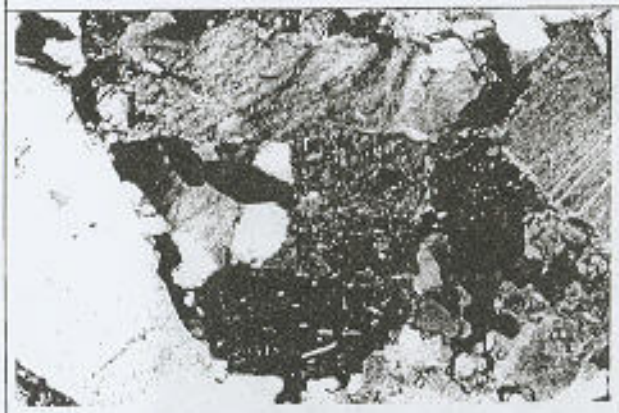

(c) Microphotograph showing apatite and zircon in diorite. C.N. X=20

(d) Microphotograph showing Fludial texture, in metabasalts C.N. X=25

(e) Microphotograph showing plagioclase microlaths and tremolite n metabasalts C.N. X=25

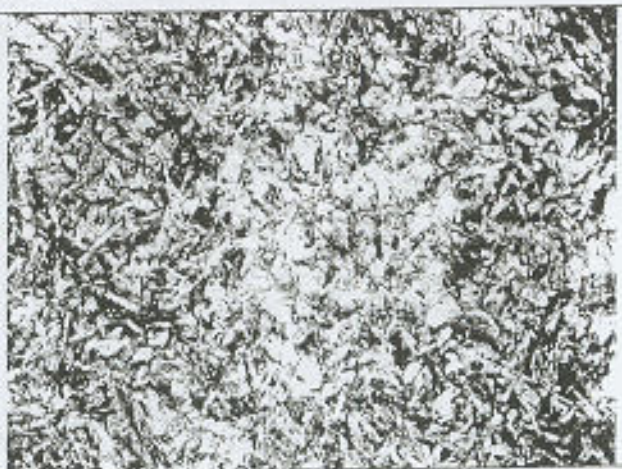

(f) Microphotograph showing plagioclase microlaths, actinolite chlorite and epidote in meta-andesites C.N. X=25

Figure (3)

(a) Microphotograph showing euhedral crystal of orthoclase microperthite and hornblende in alkaline syenites (outer ring) C.N. X=10

(b) Microphotograph showing aegrine in alkaline syenites . (Outer ring) P.L. X=10

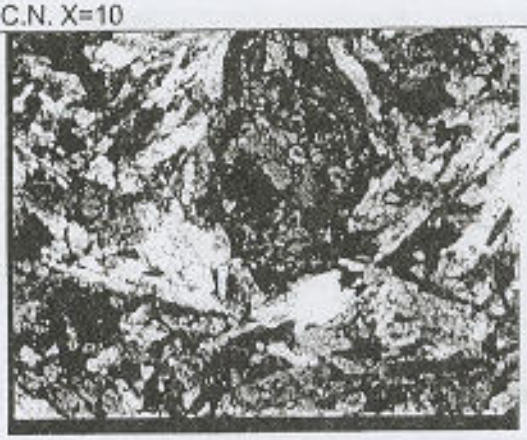

(c) Microphotograph showing zircon and apatite in alkaline syenites . (outer ring) C.N. X=20

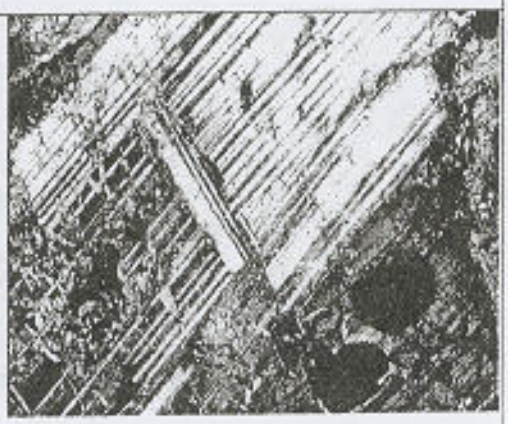

(d) Microphotograph showing plagioclase and flaky biotite in (Outer ring) . C.N. X=25

(e) Microphotograph showing antiperthite in alkaline syenites . (Inner ring) C.N. X=25

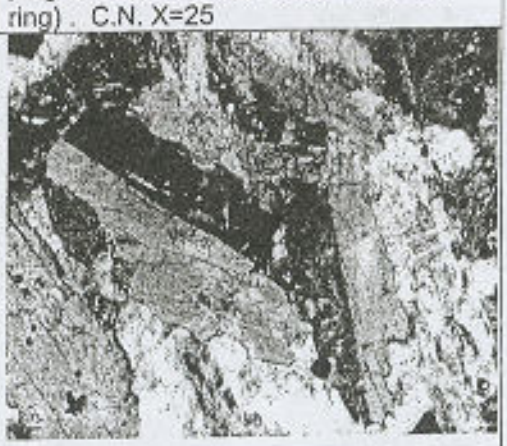

(f) Microphotograph showing simple twinning in hornblende in alkaline syenites . (Outer ring) C.N. X=25

Figure (4)

The ferromagnesian minerals are mainly titaniferous augite, aegirine-augite and iron oxides (Fig: 5-b). The accessory minerals are mainly represented by apatite and few sphene grains.

**3 - The Central Stock**

The central stock is represented by Hb- gabbros, trachybasalt and small bodies of essexite diabases which are hypabyssal equivalent of essexite gabbros and trachybasalt. The essexite gabbros are coarse to medium grained with light greyish to greenish colour. Microscopically they have hypidiomorphic to panidiomorphic texture and they mainly consist of cumulus plagioclase, amphiboles (mainly hornblende) and pyroxenes (titanoaguite replaced by aegirine-augite and others dark minerals) (Fig: 5-f), while chlorite and biotite are present as secondary alteration products (Fig: 5-e). Opaques, apatite and sphene are accessories.

The most common accessory minerals present in the studied rocks are zircon, (Fig.6) apatite (Fig. 7), ilmenite (Fig. 8) and magnetite (Fig. 9).

According to the textural characteristic, (Tuttle and Bowen 1958, Greenberg 1981), the studied syenitic rocks are characterized by the presence of perthitic feldspar and plagioclase feldspar which means that they are subsolvus. Also, modal analysis of the studied rocks are shown in table (1) and plotted graphically in QAP diagram after IUGS (1979) and Streckeisen (1976) (Fig. 10). It is clear that the studied rocks plot in the syenite, and quartz syenite fields.

**Table (1) Modal analysis of Gabal El Khafa samples.**

| Sample No. | Outer ring | | | | | Inner ring | | | | |
|---|---|---|---|---|---|---|---|---|---|---|
| | Kh-13 | Kh-14 | Kh-15 | Kh-16 | Kh-17 | Kh-7 | Kh-8 | Kh-9 | Kh-11 | Kh-12 |
| Quartz | 4.1 | 5.7 | 5.0 | 3.0 | 5.1 | 3.0 | 5.3 | 2.9 | - | - |
| Perthite-orthoclase | 72.0 | 73.2 | 71.2 | 75.1 | 74.9 | 76.9 | 74.0 | 75.4 | 83.2 | 81.0 |
| Plagioclase | 12.9 | 12.5 | 13.4 | 11.9 | 11.2 | 9.5 | 10.2 | 10.0 | 7.5 | 8.1 |
| Augite-Aegirine augite | 8.2 | 6.6 | 7.3 | 8.4 | 6.9 | 8.6 | 8.5 | 9.8 | 5.8 | 6.9 |
| Nepheline | - | - | - | - | - | - | - | - | 0.9 | 1.3 |
| Hornblende &Biotite | 0.7 | 0.5 | 0.3 | 0.3 | 0.2 | - | - | - | 1.5 | 1.2 |
| Accessory | 2.1 | 1.5 | 2.5 | 1.3 | 1.7 | 2.0 | 2.0 | 1.9 | 1.1 | 1.5 |

**General Chemical characteristics of the studied rock units**

Seven samples representing the country rocks (3 diorites and 4 metavolcanics samples) , six samples representing the alkali syenites of the outer ring, four samples from the alkali syenites and two samples from the nepheline syenite of the inner ring and two samples representing essexite

(a) Microphotograph showing aegrine augite and iron oxides in nepheline syenite . (inner ring) P.L. X=20

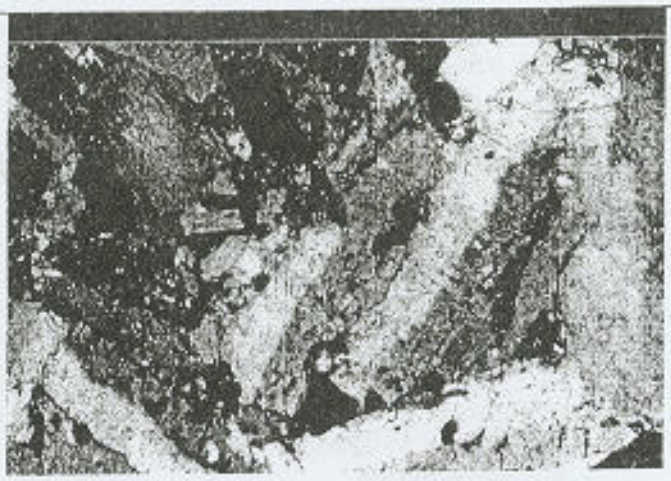

(b) Microphotograph showing nepheline associated with biotite in nepheline syenite (inner ring) C.N. X=10

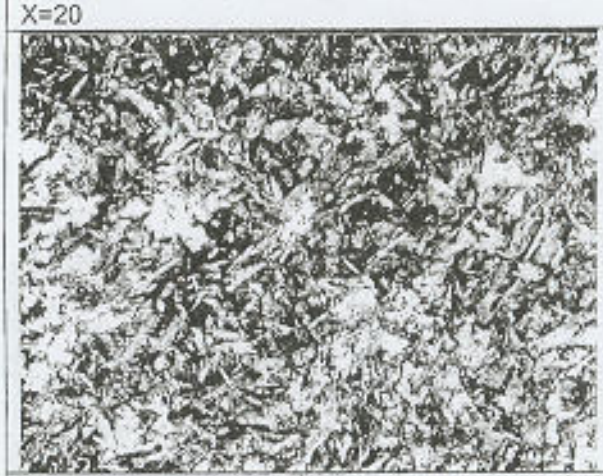

(c) Microphotograph showing fine crystal of K-feld. and agerine in essexite gabbros . C.N. X=20

(d) Microphotograph showing biotite in essexite gabbros C.N. X=25

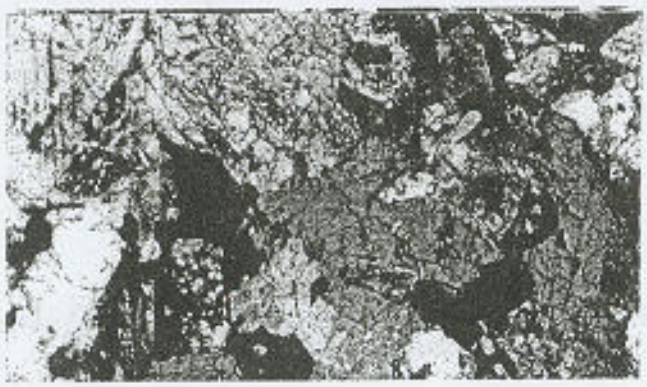

(e) Microphotograph showing Hb and pyroxene in essexite gabbros C.N. X=25

Figure (5)

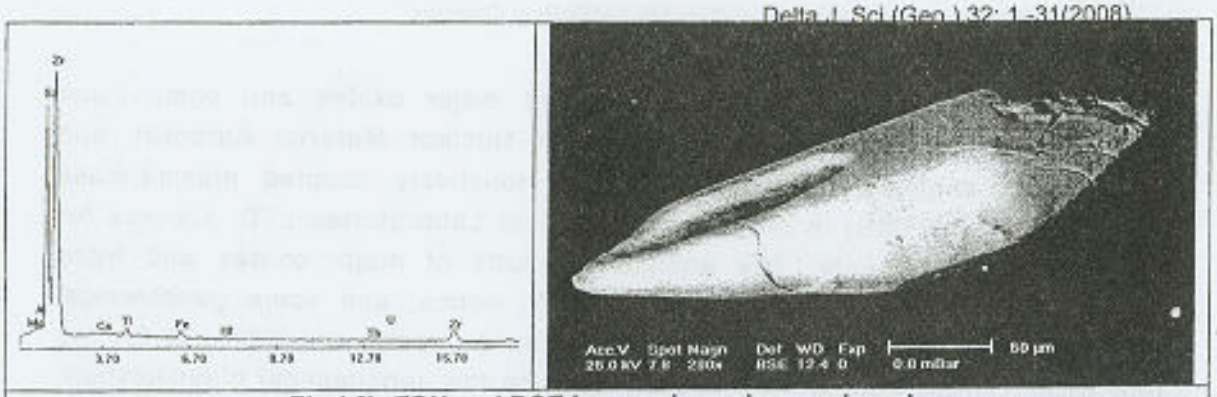


Fig.( 6): EDX and BSE image show zircon mineral.

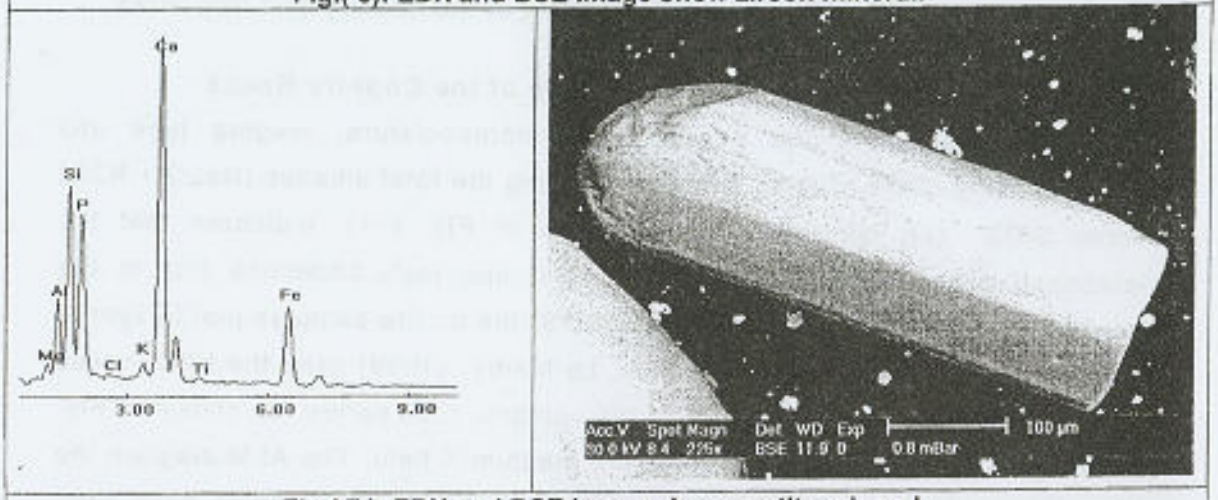


Fig.( 7 ): EDX and BSE image show apatite mineral.

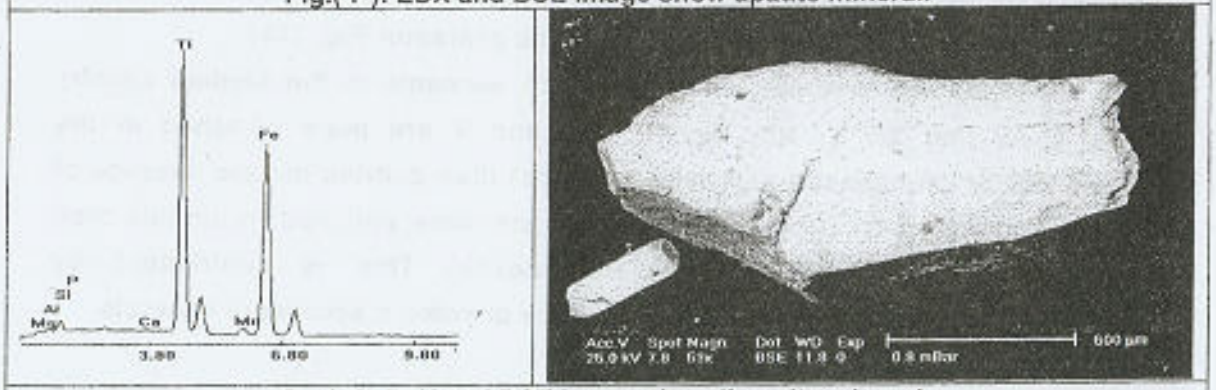


Fig.( 8): EDX and BSE image show ilmenite mineral.

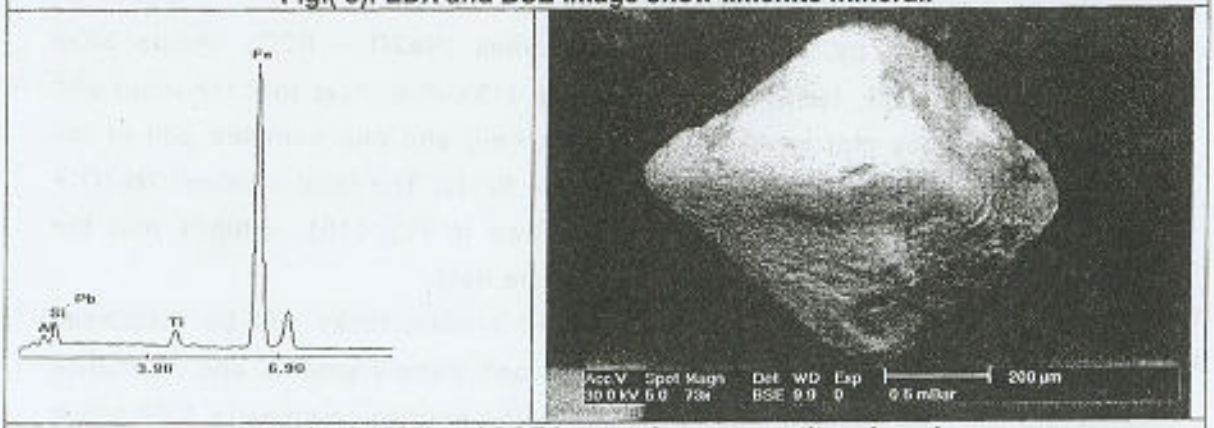


Fig.( 9 ): EDX and BSE image show magnetite mineral.

gabbro of the central stock were analyzed major oxides and some trace elements in the Analytical Laboratories of Nuclear Material Authority and someof the samples were analyzed by inductively coupled plasma-mass spectrometry (ICP-MS) in the ACME Analytical Laboratories LTD, Canada for trace and RE elements. The analytical results of major oxides and trace elements along with the calculated C.I.P.W. norms, and some geochemical parameters are given in Table (2) for the country rocks and table (3) for the ring rocks. These data will be used to discuss the geochemical classification, magma type, tectonic setting and petrogenesis of the country and ring rocks.

**1- Chemical Classification and Magma Type of the Country Rocks**

From Table (2) the petrochemical nomenclature, magma type and tectonic setting of the studied samples by using the total alkalies (Na2O + K2O) versus SiO2 (Le Maitre 1989) as shown in Fig. (11), indicates that the metabasalt samples plot in the basalt field and meta-andesites plot in the andesite field. According to Cox et al., (1979) the diorite samples plot in syeno-diorite field as shown in Fig. (12). Also, Le Maitre, (1989) used the K2O versus SiO2 relationship in order to classify the volcanic rock series, as shown in Fig. (13) Where the studied samples lie in the medium-K field. The AFM diagram the studied samples show that the diorite and meta-andesite samples have calc-alkaline but metabasalt samples have tholeiitic character Fig. (14).

The average distributions of the trace elements in the studied country rocks show that Zr, Y, Nb, Ba, Ni, Co, and V are more enriched in the metavolcanics (metabasalt and meta-andesite) than diorites but the average of the trace elements Sr, Rb, Cu, Cr and Zn are more enriched in diorites than metavolcanics (metabasalt and meta-andesite) This is contributed by differentiation of the magma and the presence of some a accessory minerals

2-**Geochemistry** of the ring rocks:-

The geochemical classification, and nomenclature of the ring rocks can be determined by by using The total alkalies (Na2O + K2O) versus SiO2 diagram (Middlemost, 1985) as shown in Fig. (15). It is clear that the inner and outer ring samples plot in alkali Qz syenite field and one samples poit in the quartz syenite and other in quartz monzonite fields. The total alkalies (Na2O + K2O) versus SiO2 (Le Maitre 1989) as shown in Fig. (16), exhibits that the inner and outer ring samples plot in the syenite field.

The magma type of the investigated syenite rocks will be discussed using some geochemical parameters, major and trace elements and normative compositions. The average agpaitic index in the studied samples is 1.09 which means that they are agpatic in nature which explains the formation of alkaline

minerals like aegirine (Goldschmidt, 1954).Also from the variation diagrams, of major elementsSiO2 –Na2O+K2O Irvine and Baragar, (1971) it is clear that the most of the studied syenite samples have alkaline character Fig. (17).

The AFM diagram (Irvine and Baragar, 1971) figure (18)show that the studied syenite samples plot in calc-alkaline field and the samples show a trend parallel to the extension regime of the Petro et al.(1979).

The Al2O3/(Na2O+K2O) - Al2O3/(CaO+Na2O+K2O) diagram figure (19) show that the studied samples were generated from peralkaline magma.

In order to determine the tectonic setting of emplacement, several diagrams based on the trace elements concentration are used.

A number of major and trace element variation diagrams are used to provide useful information about the nature of the tectonic regimes within which magmas were generated. Maniar and Piccoli, (1989) discriminated the tectonic setting of the granitoid rocks based on their major elements chemistry. They dicriminated the oceanic plagiogranite (OP) from all other granitoids by using the K2O versus SiO2 plot shown in (Fig.20) the studied samples plot outside the oceanic plagiogranite field. Discrimination between group I subduction related granites (island arc granitoids + continental collision granitoids + continental arc granitoids), group II rift related granites (rift–related granitoids + continental epeirogenic uplift granitoids) and group III granites (post orogenic granitoids) can be achieved by using Feo*/FeO+MgO versus SiO2 diagram as shown in (Fig. 21) where the studied samples plot in RRG + CEUG field. Also the discrimination between rift-related granitoids and continental epeirogenic uplift granitoids can be achieved by the TiO2 Plot as shown in Fig. (22) Where the studied samples plot in the continental epeirogenic uplift granitoids. Also, it is associated with continental areas, which have experienced epeirogenic crustal uplift with no subsequent development of a rift. This uplift is possibly due to hot spot activity or an aborted rifting event.

The variation diagram of Nb-Y Pearce et al. (1984) is used to discriminate between oceanic ridge granite which is enriched in Y contents and volcanic arc and collision granites which are depleted in Y as shown in (Fig. 23). The data of the studied samples plot in the within- plate field.

The variation diagram Rb-(Y+ Nb) Pearce et al. (1984) is used to discriminate between volcanic arc granites depleted in Rb contents and collision granites enriched in Rb as shown in (Fig.24). The studied samples lie in the within-plate granite field. This indicates that the studied samples are developed in within plate tectonic setting.

able (2):- Chemical analysis of major and trace elements of the countary rocks of Gabal El Kahafa ring complex.

| Rock type | Diorite | | | Metavolcanics | | | |
|---|---|---|---|---|---|---|---|
| | | | | Metabasalt | | Meta-andesite | |
| Sample No. | Kh-1 | Kh-2 | Kh-3 | Kh-4 | Kh-4/ | Kh-5 | Kh-5/ |
| $SiO_2$ | 60.52 | 62.13 | 62.18 | 48.70 | 49.30 | 61.21 | 60.93 |
| $TiO_2$ | 0.71 | 0.44 | 0.24 | 0.93 | 1.10 | 1.15 | 0.95 |
| $Al_2O_3$ | 15.90 | 16.19 | 16.01 | 16.10 | 16.20 | 16.60 | 15.61 |
| $Fe_2O_3$ | 1.31 | 1.39 | 1.29 | 4.50 | 3.35 | 3.72 | 3.25 |
| FeO | 5.01 | 4.51 | 4.52 | 7.10 | 7.93 | 3.70 | 3.81 |
| MnO | 0.19 | 0.14 | 0.21 | 0.25 | 0.23 | 0.12 | 0.18 |
| MgO | 0.45 | 1.34 | 1.14 | 3.65 | 4.23 | 2.18 | 2.93 |
| CaO | 5.36 | 4.75 | 4.93 | 8.69 | 8.40 | 3.35 | 3.68 |
| $Na_2O$ | 6.24 | 4.89 | 5.40 | 3.20 | 3.31 | 3.15 | 3.41 |
| $K_2O$ | 3.25 | 2.78 | 3.01 | 1.30 | 0.98 | 1.35 | 1.41 |
| $P_2O_5$ | 0.21 | 0.28 | 0.31 | 0.35 | 0.30 | 0.22 | 0.25 |
| L.O.I. | 0.80 | 0.79 | 0.81 | 4.92 | 4.64 | 3.11 | 3.29 |
| Total % | 99.95 | 99.63 | 100.05 | 99.70 | 99.97 | 99.86 | 99.88 |
| C.I.P.W.norm | | | | | | | |
| Qz | 1.15 | 10.42 | 7.20 | 1.60 | 0.99 | 27.84 | 23.53 |
| Or | 19.39 | 16.64 | 17.94 | 8.11 | 6.08 | 8.25 | 8.65 |
| Ab | 53.19 | 41.81 | 45.99 | 28.54 | 29.35 | 27.52 | 29.89 |
| An | 5.79 | 14.14 | 10.60 | 27.10 | 27.71 | 15.85 | 17.43 |
| Di | 16.26 | 6.81 | 10.42 | 13.38 | 11.72 | 0.00 | 0.00 |
| Hy | 0.00 | 6.67 | 4.82 | 11.71 | 16.19 | 7.74 | 10.78 |
| Wo | 0.49 | 0.00 | 0.00 | 0.00 | 0.00 | 0.00 | 0.00 |
| Cor | 0.00 | 0.00 | 0.00 | 0.00 | 0.00 | 4.47 | 2.39 |
| Mt | 1.92 | 2.04 | 1.88 | 6.89 | 5.10 | 5.58 | 4.89 |
| Il | 1.36 | 0.85 | 0.46 | 1.86 | 2.19 | 2.26 | 1.87 |
| Ap | 0.46 | 0.62 | 0.68 | 0.81 | 0.69 | 0.50 | 0.57 |
| Trace elements | | | | | | | |
| Zr | 415 | 430 | 461 | 542 | 529 | 528 | 539 |
| Y | 34 | 37 | 41 | 40 | 38 | 46 | 44 |
| Sr | 410 | 435 | 476 | 391 | 401 | 318 | 334 |
| Rb | 55 | 46 | 51 | 34 | 31 | 32 | 29 |
| Nb | 18 | 20 | 16 | 73 | 68 | 57 | 53 |
| Ba | 615 | 713 | 690 | 960 | 905 | 880 | 893 |
| Cu | 64 | 73 | 80 | 62 | 58 | 60 | 61 |
| Ni | 12 | 10 | 11 | 28 | 30 | 25 | 23 |
| Co | 9 | 6 | 8 | 10 | 11 | 15 | 13 |
| Cr | 45 | 42 | 43 | 30 | 31 | 25 | 24 |
| V | 18 | 13 | 15 | 21 | 22 | 19 | 18 |
| Zn | 75 | 63 | 69 | 39 | 38 | 43 | 39 |

Table(1):Chemical analysis of major and trace elements of Gabal El Khafa ring complex

| S.No. | Central Stock | | Inner Ring | | | | Hypo Syenite | | Outer Ring | | | | | |
|---|---|---|---|---|---|---|---|---|---|---|---|---|---|---|
| | Gabbro | | Alkaline syenite | | | | | | Alkaline syenite | | | | | |
| | Kh-6 | Kh-6/ | Kh-7 | Kh-8 | Kh-9 | Kh-10 | Kh-11 | Kh-12 | Kh-13 | Kh-14 | Kh-15 | Kh-16 | Kh-17 | Kh-18 |
| $SiO_2$ | 47.64 | 47.35 | 64.32 | 64.87 | 64.55 | 64.01 | 61.1 | 62 | 65.24 | 65.05 | 64.64 | 63.9 | 65.41 | 64.1 |
| $TiO_2$ | 1.98 | 1.87 | 0.52 | 0.42 | 0.49 | 0.36 | 0.71 | 0.68 | 0.42 | 0.63 | 0.72 | 0.6 | 0.4 | 0.69 |
| $Al_2O_3$ | 20.55 | 21.2 | 13.9 | 13.86 | 13.31 | 13.8 | 16.5 | 18.01 | 14.1 | 14.28 | 14.8 | 14.41 | 14.1 | 14.5 |
| $Fe_2O_3$ | 7.56 | 6.98 | 3.25 | 2.4 | 2.35 | 2.3 | 5.65 | 1.25 | 3.25 | 2.45 | 2.03 | 3.5 | 4.26 | 2.3 |
| FeO | 6.3 | 6.13 | 2.2 | 2.9 | 3.12 | 4.01 | 3.5 | 3.01 | 3.23 | 2.25 | 3.38 | 3.85 | 2.35 | 3.11 |
| MnO | 0.23 | 0.19 | 0.18 | 0.1 | 0.15 | 0.13 | 0.21 | 0.15 | 0.12 | 0.17 | 0.14 | 0.15 | 0.16 | 0.14 |
| MgO | 0.83 | 0.98 | 0.8 | 1.31 | 1.13 | 1.2 | 1.41 | 0.96 | 0.8 | 0.92 | 0.61 | 0.84 | 0.6 | 0.72 |
| CaO | 9.58 | 10.13 | 2.35 | 2.4 | 1.45 | 1.69 | 2.8 | 1.4 | 0.86 | 0.56 | 1.12 | 1.69 | 1.4 | 1.1 |
| $Na_2O$ | 2.6 | 2.85 | 6.78 | 6.7 | 6.75 | 7.29 | 3.8 | 7.81 | 7.43 | 6.98 | 7.01 | 6.65 | 5.8 | 6.58 |
| $K_2O$ | 1.43 | 1.6 | 5.13 | 5.1 | 4.39 | 3.32 | 4.29 | 4.13 | 4.11 | 4.3 | 4.28 | 5.33 | 4.1 | 4.25 |
| $P_2O_5$ | 0.18 | 0.21 | 0.33 | 0.08 | 0.13 | 0.25 | 0.2 | 0.19 | 0.13 | 0.18 | 0.14 | 0.18 | 0.12 | 0.16 |
| L.O.I. | 0.78 | 0.65 | 3.2 | 1.44 | 2.87 | 3.53 | 3.36 | 1.25 | 1.28 | 1.64 | 1.76 | 1.43 | 1.08 | 1.53 |
| Total% | 100.83 | 99.99 | 99.66 | 100.38 | 99.84 | 99.79 | 99.63 | 100.1 | 100.5 | 99.61 | 100.44 | 100.53 | 100.58 | 100.02 |
| C.I.P.W norm | | | | | | | | | | | | | | |
| Qz | 5.62 | 2.5 | 5.89 | 6.64 | 6.28 | 5.43 | 0 | 0 | 6.56 | 7.8 | 5.22 | 4.15 | 8.89 | 6.5 |
| Or | 8.52 | 9.53 | 30.82 | 30.52 | 26.1 | 19.8 | 25.82 | 24.71 | 24.5 | 25.95 | 25.65 | 30.59 | 24.37 | 24.8 |
| Ab | 23.14 | 24.26 | 45.48 | 45.27 | 48.23 | 54.43 | 54.58 | 59.84 | 45.9 | 58.41 | 53.87 | 45.95 | 49.83 | 48.82 |
| An | 40.37 | 40.55 | 0 | 0 | 0 | 0 | 5.22 | 5.5 | 0 | 0 | 0 | 0 | 0 | 0 |
| Acm | 0 | 0 | 9.53 | 7.01 | 6.98 | 6.36 | 0 | 0 | 9.13 | 7.22 | 5.94 | 9.41 | 6.99 | 7.12 |
| Ns | 0 | 0 | 0.91 | 1.41 | 0.86 | 0.14 | 0 | 0 | 0.1 | 0.38 | 0.3 | 0 | 0 | 0.13 |
| Di | 7.06 | 7.14 | 4.58 | 5.54 | 5.73 | 5.89 | 6.45 | 0.34 | 2.93 | 1.47 | 4.12 | 6.27 | 5.24 | 5.18 |
| Hy | 1.08 | 1.58 | 3.28 | 4.62 | 6.28 | 7.1 | 4.12 | 5.7 | 5.95 | 4.75 | 4.38 | 1.54 | 0.94 | 3.41 |
| Ol | 0 | 0 | 0 | 0 | 0 | 0 | 1.44 | 0.26 | 0 | 0 | 0 | 0 | 0 | 0 |
| Mt | 11.83 | 10.23 | 0 | 0 | 0 | 0 | 0.96 | 1.83 | 0 | 0 | 0 | 0.33 | 2.3 | 4.66 |
| Il | 3.75 | 3.58 | 1 | 0.81 | 0.62 | 0.74 | 1.37 | 1.31 | 0.8 | 1.61 | 1.41 | 1.15 | 0.76 | 0.67 |
| Ap | 0.4 | 0.46 | 0.51 | 0.18 | 0.28 | 0.55 | 0.44 | 0.42 | 0.29 | 0.4 | 0.31 | 0.35 | 0.26 | 0.28 |
| Trace Elements: | | | | | | | | | | | | | | |
| Zr | 190 | 178 | 648.3 | 900 | 852.8 | 941.5 | 1046 | 637.8 | 641 | 1695 | 395 | 588.5 | 801 | 652 |
| Y | 18 | 21 | 55.9 | 60 | 73.1 | 65.3 | 68.7 | 65.8 | 46 | 72.8 | 35 | 35.9 | 46 | 61 |
| Sr | 315 | 286 | 396.1 | 293 | 389.8 | 348.2 | 525.8 | 526.5 | 188 | 86 | 278 | 948.7 | 258 | 301 |
| Rb | 49 | 54 | 83 | 79 | 94.5 | 91.3 | 89.4 | 87.6 | 108 | 175 | 115 | 35.3 | 68 | 71 |
| Nb | 18 | 19 | 165.3 | 163 | 225 | 215 | 211.9 | 203.7 | 133 | 289 | 81 | 62 | 119 | 125 |
| Ba | 385 | 293 | 730.6 | 614 | 712.8 | 986 | 903.6 | 921 | 369 | 150.8 | 239 | 578 | 513 | 410 |
| Cu | 29 | 32 | 11 | 12 | 8.7 | 9.2 | 9.1 | 11.4 | 13 | 14.3 | 11 | 16.7 | 35 | 14 |
| Ni | 13 | 9 | 4.4 | 6 | 3.7 | 4.3 | 3.5 | 4.3 | 5 | 4.5 | 6 | 8.1 | 7.1 | 6.6 |
| Co | 18 | 8 | 6.1 | 8 | 5.7 | 6.3 | 6.6 | 6.7 | 5 | 1.3 | 4 | 15.4 | 7.3 | 6.9 |
| Cr | 365 | 370 | 23 | 27 | 19 | 23 | 21 | 28 | 28 | 20 | 21 | 25 | 18 | 23 |
| Mo | 4 | 4.2 | 3.8 | 9 | 4.5 | 3.6 | 3.3 | 3.1 | 4 | 2.1 | 5 | 2.1 | 8 | 6.9 |
| Sc | | | 9 | 12 | 11 | 10 | 11 | 10 | 12 | 16 | 10 | 2 | 7 | 8 |
| K/Rb | 214 | 246 | 526 | 515 | 385 | 284 | 398 | 392 | 316 | 204 | 312 | 1193 | 503 | 501 |
| K/Ba | 19.6 | 45.4 | 58 | 69 | 53 | 26 | 44.5 | 41.8 | 203 | 236 | 148.5 | 185 | 66.3 | 87 |
| Ba/Rb | 8.23 | 5.43 | 8.89 | 7.7 | 7.57 | 10.84 | 8.86 | 9.37 | 1.56 | 0.86 | 2.22 | 10.34 | 7.54 | 5.77 |
| Rb/Sr | 0.15 | 0.19 | 0.2 | 0.27 | 0.31 | 0.27 | 0.28 | 0.27 | 0.57 | 2.03 | 0.42 | 0.04 | 0.31 | 0.24 |
| U | 3.9 | 3.1 | 3.9 | 8.1 | 7.3 | 8.2 | 3.6 | 3.1 | 7.9 | 10.5 | 23 | 1.9 | 3.6 | 4.3 |
| Th | 5.45 | 6.41 | 16.5 | 38.2 | 28.1 | 31.5 | 12.6 | 30.2 | 24.9 | 32.7 | 9.1 | 7.2 | 14 | 16.5 |
| Th/U | 1.4 | 2.7 | 4.23 | 3.73 | 3.65 | 3.8 | 3.5 | 3.29 | 3.15 | 3.11 | 3.96 | 3.79 | 3.89 | 4.02 |
| La | | | 87.1 | 123 | 107.4 | 133 | 105.3 | 103.6 | 128 | 123.1 | 78.1 | 59.5 | 80 | 87.1 |
| Ce | | | 174.6 | | 224.3 | | 215.2 | 195.9 | | 228.5 | | 125.8 | | |
| Pr | | | 18.48 | | 24.43 | | 23.27 | 22.44 | | 23.51 | | 14 | | |
| Nd | | | 72.1 | | 94.6 | | 93.8 | 89.7 | | 68.9 | | 59.8 | | |
| Sm | | | 13.9 | | 17.6 | | 16.6 | 17 | | 11.9 | | 11.2 | | |
| Eu | | | 3.15 | | 3.25 | | 3.33 | 3.42 | | 3.05 | | 3.46 | | |
| Gd | | | 12.2 | | 15.44 | | 15 | 14.58 | | 9.24 | | 9.34 | | |
| Tb | | | 2.09 | | 2.64 | | 2.37 | 2.36 | | 1.97 | | 2.34 | | |
| Dy | | | 10.35 | | 14.06 | | 13.89 | 13.82 | | 11.14 | | 6.97 | | |
| Ho | | | 3.88 | | 2.44 | | 2.4 | 2.32 | | 2.18 | | 1.43 | | |
| Er | | | 4.83 | | 6.64 | | 6.24 | 5.87 | | 6.3 | | 2.95 | | |
| Tm | | | 0.7 | | 0.99 | | 0.89 | 0.87 | | 1 | | 0.41 | | |
| Yb | | | 4.43 | | 5.68 | | 5.45 | 5.81 | | 6.84 | | 2.34 | | |
| Lu | | | 0.57 | | 0.72 | | 0.77 | 0.68 | | 0.9 | | 0.31 | | |

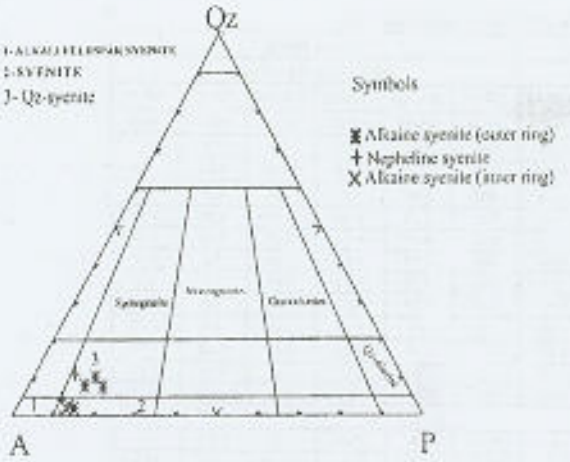


Fig.(10): Q- A- P diagram (Streckeisen, 1973).

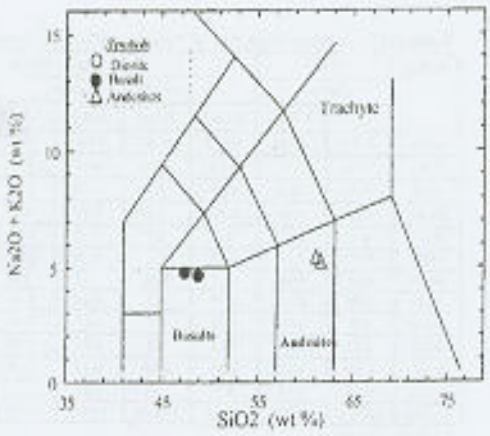


Fig.(11): $(Na_2O+K_2O)$-$SiO_2$ (Le Maitre, 1989).

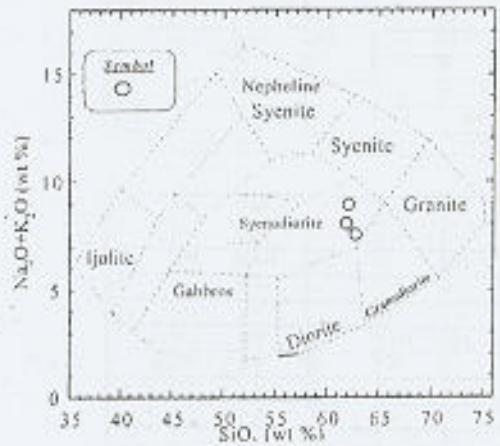


Fig. (12): The total alkalies versus SiO2 (TAS) diagram of Cox et al., (1986).

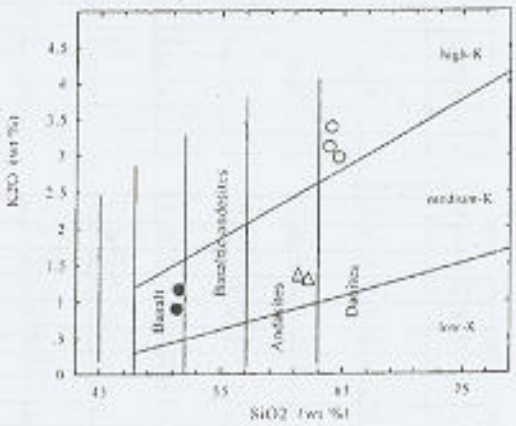


Fig. (13) : $K_2O$-$SiO_2$ (Le Maitre, 1989).

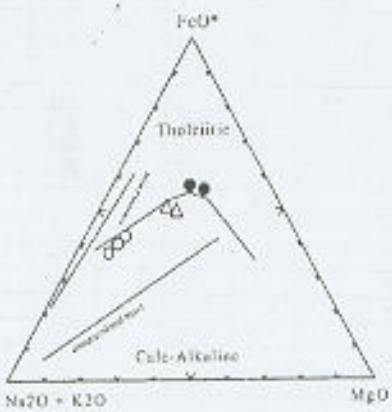


Fig.(14) :AFM diagram, (Irvine and Baragar, 1971).

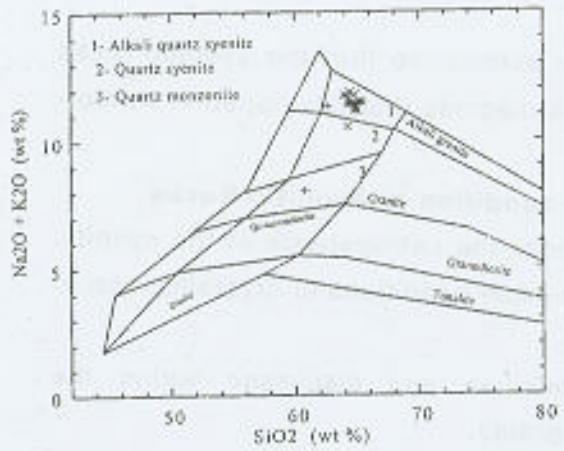


Fig. (15): $SiO_2$-($Na_2O$+$K_2O$) diagram (Middlemost, 1985)

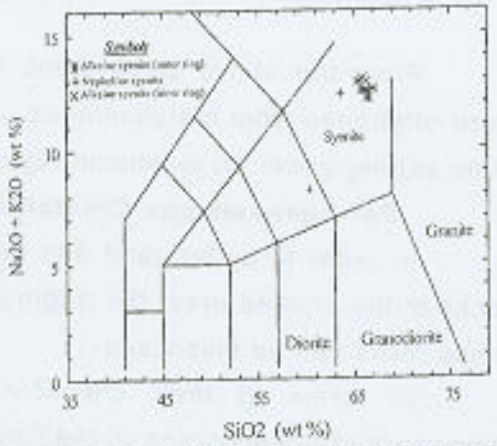


Fig. (16): ($Na_2O$+$K_2O$)-$SiO_2$ (Le Maitre,1989).

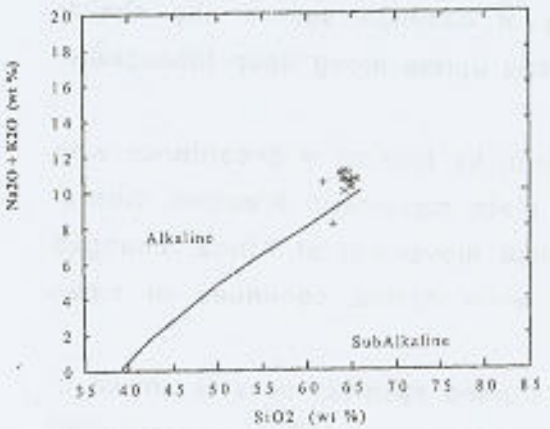


Fig. (17): ($Na_2O$+$K_2O$)-$SiO_2$ (Irvine and Baragar,1971).

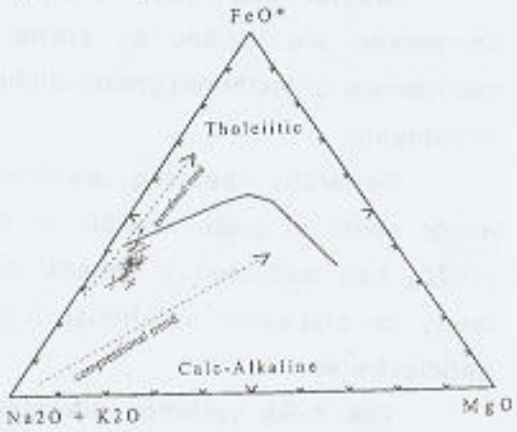


Fig. (18):AFM diagram, (Irvine and Baragar, 1971)

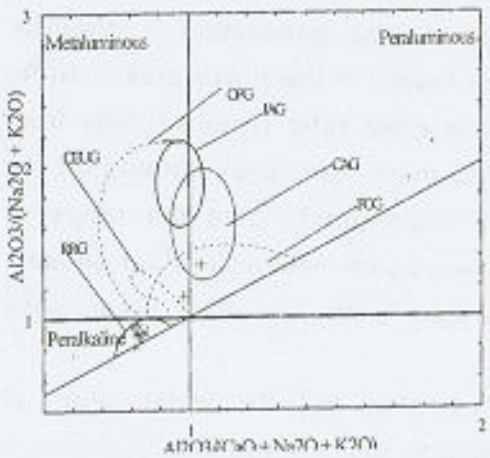


Fig. (19): Shand index (Maniar and piccoli 1989).

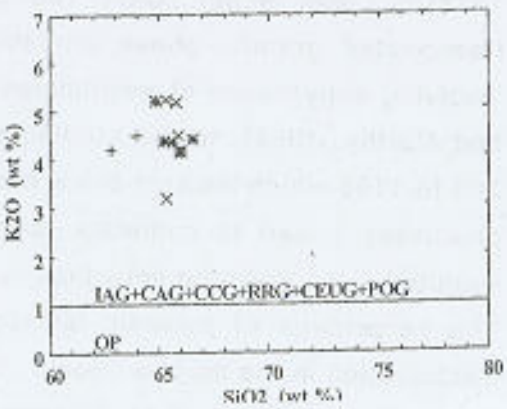


Fig. (20): SiO2-K2O (Maniar and piccoli 1989).

From the above discussions we can summarize that the syenitic rocks were originated from metaluminous alkaline magmas that developed in within - plate setting under an extension regime.

**Petrogenesis and Crystallization condition of Syenitic Rocks**

In order to understand and determined the petrogenesis of the syenitic rocks of the studied area, the origin and possible conditions of crystallization of these rocks can be discussed

in terms of their chemical composition and discussed within the framework of the evolution of the Egyptian Shield.

Gruyter and Vogel (1981) suggest that the Egyptian alkaline ring complexes are formed by partial melting of common source and similar mechanism of asthenospheric disturbance and uprise along deep lithospheric lineaments.

Generally speaking, alkaline suites can be formed in accordance with major shifts in plate velocity or shifts in plate movement direction. Girdler (1970) has indicated a general anticlockwise movement of Africa, changed lately to clockwise rotational movement, while Arabia continued to move anticlockwise.

The K-Rb variation diagram of the studied syenitic rocks is shown in (Fig. 25). The average values of studied syenites equal 462which are higher than the crustal average value of 250 (Taylor, 1965). The higher K/Rb ratio indicates sources regions for magma generation in the lower crust (Heier, 1973) or upper mantle (Gast, 1965). Also, the higher K/Rb ratios for the more fractionated granitic phase probably indicate magma generation mechanism involving dehydration of amphiboles at deeper levels in the lower crust (Griffin and Murthy, 1969). In the studied samples the K/Rb ratio rises strongly from 204 to 1193 which indicate the K mobile and Rb inert. This investigated that the processes linked to cumulate formation are important to give the range of syenites in an environment which is homogeneous with respect to fluid phases. The percentage of potassic feldspar in the rock is the result of plagioclase fractionation in the magma (Bonin, 1986).

The Rb/Sr variation diagram is shown in (Fig. 26). The most values of Rb/Sr of studied samples are < 0.5 which indicates that the syenites rocks were generated from more evolved magmatic fluids.This indicate that the action of magmatic liquid on trace element behaviour; there is early precipitation of Ba and Sr with Ca in the plagioclases followed by a residual concentration of Rb and K but without the intervention of an abundant fluid phase.

The K-Ba variation diagram is shown in (Fig. 27). The most values of K/Ba is greater than the average crustal ratios line (K/Ba=65) which indicate that they are depleted in Ba.

The Ba-Rb variation diagram shown in (Fig.28). It can be used to signify the degree of fractionation of granitoid rocks. The line representing the average Ba/Rb ratio for the crust is about (4.4) (Mason, 1966). The Ba/Rb ratios of the studied granitoid show that they have high values than the average crustal ratio that is consistent with the suggestion that these samples originated from a enriched Ba source.

Also, the environmental conditions of the syenitic rocks can be determined from the normative(Qz–Ab–Or) and (Or– Ab–An) systems as follows:-

The Qz–Ab–Or system is shown in (Fig. 29). The cotectic boundaries at 0.5 and 10kb are also shown. The studied samples are plotted in the region which indicates formation at water pressure 3-7kb at depth range from (9 -21 km) Wilson, (1989).

Figures (30) show the quartz–albite-orthoclase system illustrating the temperature isotherms. The studied samples crystallized under temperature more than 840° (James and Hamilton, 1969 and Winkler et al. 1975).

Figure (31) shows the Ab-An-Or system with the fields of rock types after O'Conner, (1965) and Barker, (1979). The effect of PH2O on the position of cotectic boundary between orthoclase and plagioclase at 1 Kb and 5Kb PH2O are also shown after Tuttle and Bowen (1958). The studied samples plot in the granite field and the magma was generated at somewhat intermediate depths equivalent to 3-6 Kb.

Crystal liquid fractionation can also produce significant changes in felsic magmas and result in chemical trends that are reverse of those produced by higher degrees of melting, i.e., less calcic granites (Bateman and Chappell, 1979). From the above it is clear that the syenitic rocks of Gabal El Kahfa Ring Complex are generated at depth of about 9-21 km equivalent to 3-6 Kb and temperature ranging from 760°c to 840°c with multi-processes of both assimilation and fractional crystallization involving plagioclases, hornblende and Fe-Ti oxides from a partial melted lithospheric magma.

From the above we can conclude that El Kahhfa massif intrudes sharply the syntectonic granitoids, while it is cut by the younger volcanics. The ring was emplaced through two main phases of activity. The first constitutes the outer part which is generally white in color and the second phase constitutes the inner ring massif which is of red color.

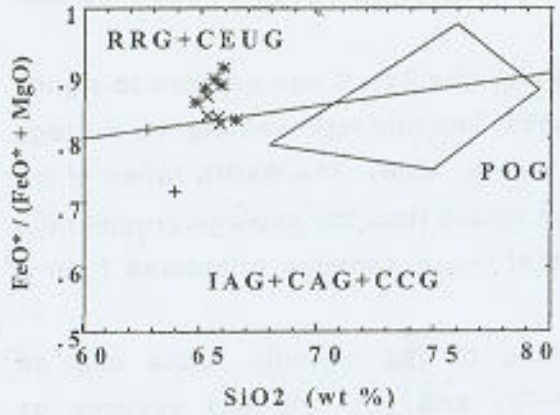


Fig. (21): SiO2-(FeO*/ FeO* + MgO) (Maniar and piccoli 1989).

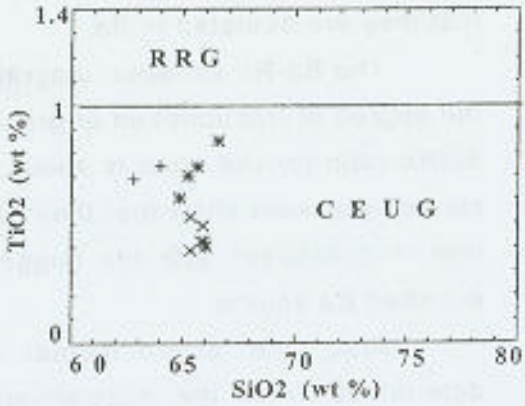


Fig. (22): SiO2-TiO2) (Maniar and piccoli 1989)

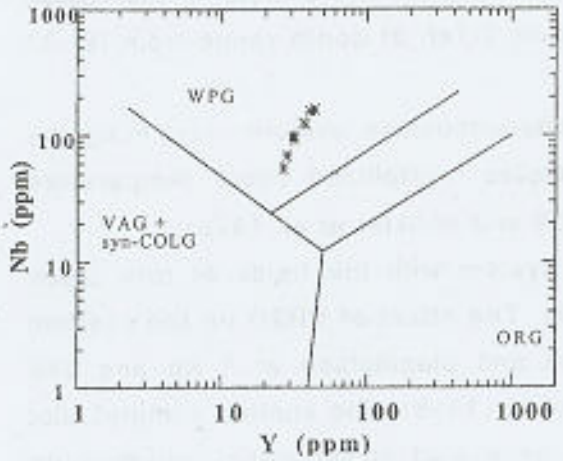


Fig. (23): Rb-(Y+Nb) Pearce et al. (1984).

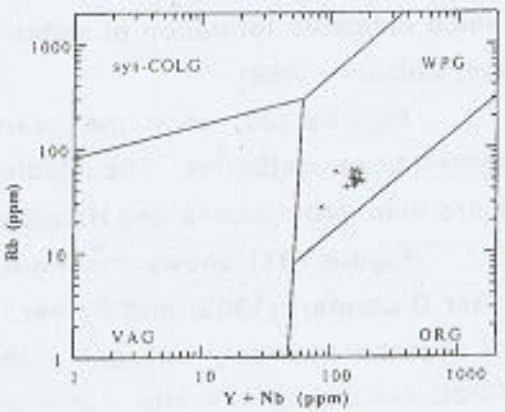


Fig. (24): Y-Nb Pearce et al. (1984).

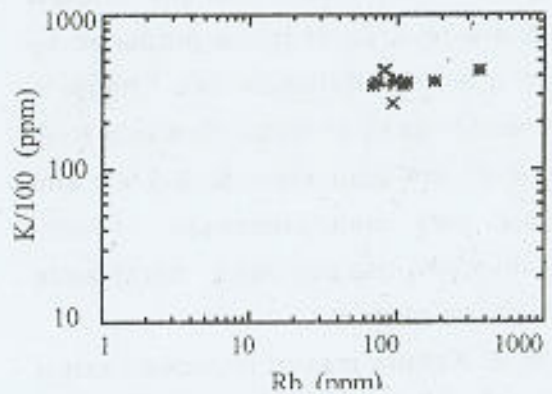


Fig. (25): Rb-( K/ 100 ) variation diagram.

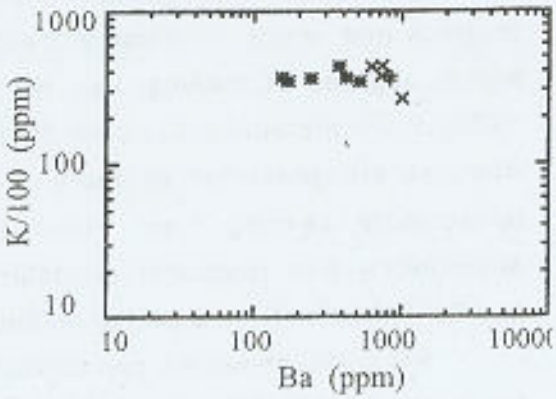


Fig. (26): Ba-( K/ 100 ) variation diagram.

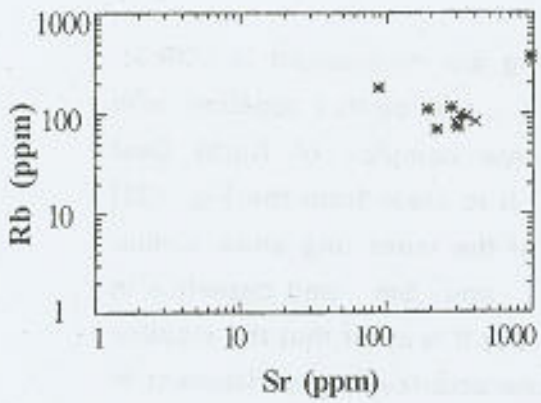


Fig.(28):Ba-Rb variation diagram.

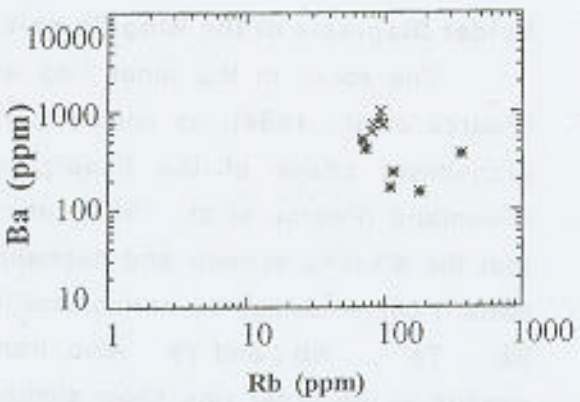


Fig. (27): Rb-Sr variation diagram.

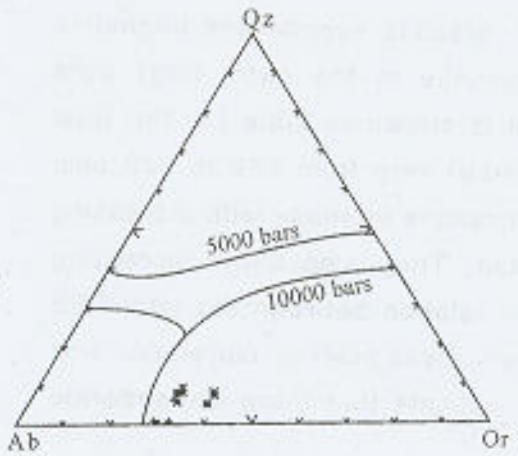


Fig. (29): Qz-Ab-Or variation diagram.

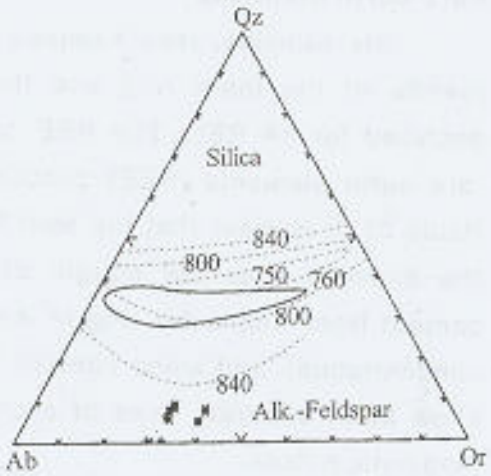


Fig (30): Qz-Ab-Or variation diagram.

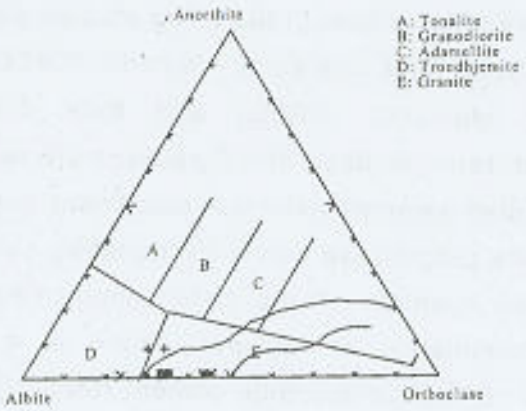


Fig. (31): Ab-An -Or variation diagram James and Hamilton (1969).

**Spider Diagrams of the Ring Complex**

The rocks in the inner ring and outer ring are normalized to (ORG), (Pearce et al., 1984), as shown in Figs.(32 &33 ) and plotted together with granophyre phase of the Skaergaard within-plate complex of North East Greenland (Pearce et al., 1984) for comparison. It is clear from the Fig. (32) that the alkaline syenite and nepheline syenite of the inner ring show similar pattern characterized by enrichment in Ba, Th and Sm and depletion in Rb , Ta , Nb , and Yb . Also, from the Fig. (33) It is clear that the alkaline syenite in the outer ring show similar pattern characterized by enrichment in Ba , Th and Sm and have average values in Rb , Ta , Nb , and Yb relative to the compared granophyre phase indicating more plagioclase fractionation

**Rare-earth elements**

Six samples, (two samples each from alkaline syenite and nepheline syenite of the inner ring and the alkaline syenite in the outer ring) were analyzed for 14 REE. The REE concentration is shown in table (3).The total rare earth elements (REE) concentrations (La-Lu) vary from 299 to 520 ppm (table 3). It is clear that the total REE concentrations increase with increasing the distance from the margin of the intrusion. They also show increasing content from the outer ring to inner ring. The relation between the total REE concentrations and silica content Fig. (34) show clear positive correlation and show three separate lines of evolution which indicate that there are separate magmatic pulses.

The chondrite-normalized REE patterns of the studied samples according to the primitive mantle (Fig. 35), is parallel and largely uniform within each lithologic unit and within the whole ring. At (Fig. 33), the normalization values are from Taylor and Mc Lennan (1985). The studied samples of the inner and outer rings show strong light rare-earth elements (LREE) enrichment over the heavy rare-earth elements (HREE) and thus display pronounced fractionation. The chondrite-normalized HREE patterns are rather flat.

Some of the studied samples exhibit a significant negative Eu anomaly (Fig.35), indicting that the plagioclase was a fractionating phase. However, four samples of the alkaline syenites of the outer, inner ring exhibit probably indicating variable accumulation of feldspar. There is a general negative correlation between the normative anorthite content (table 3) and magnitude of the negative Eu anomaly which is consistent with plagioclase fractionation. The rocks with the highest normative An-content are those with no or only slight (negative) Eu anomaly.

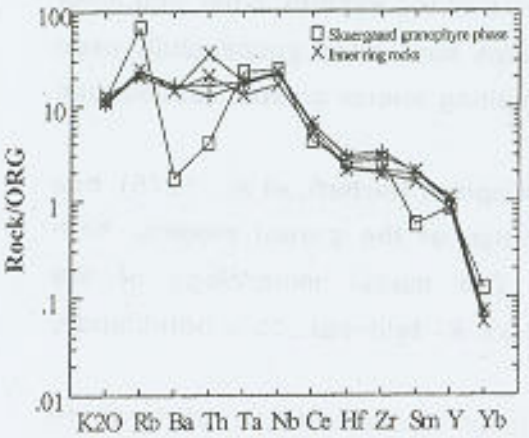


**Fig. ( 32): Spider digram for the inner ring rocks, (Pearce et al., (1984).**

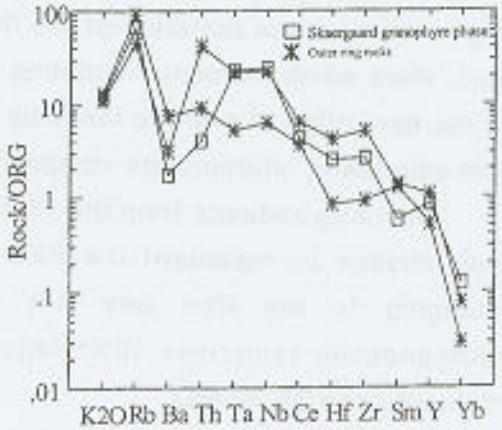


**Fig. ( 33): Spider digram for the outer ring rocks, (Pearce et al., (1984).**

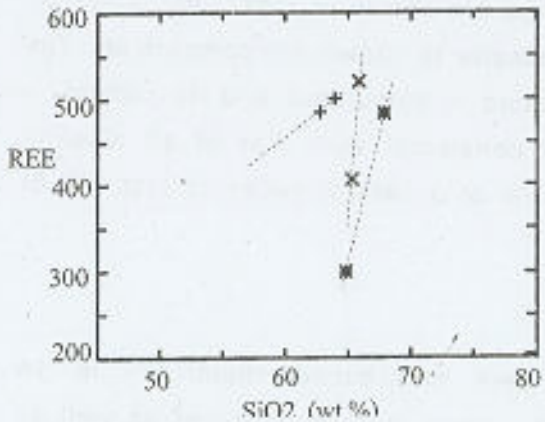


Fig. (34): Variation digram of Σ REE for the studied ring complex with $SiO_2$

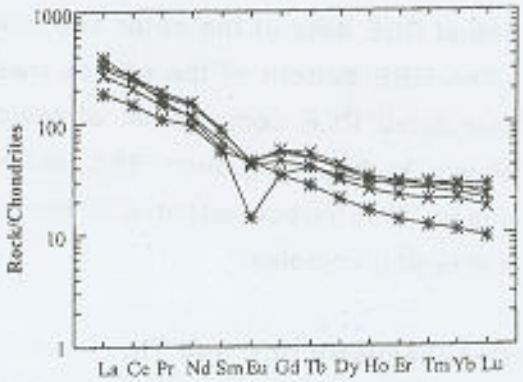


Fig. (35): Chondrites normalized REE pattern for the inner and outer ring rocks (Sun,1980)

Field evidence suggested that El Kahfa ring complex developed within large trachytic volcano; remnants of such material are still preserved. This fact would place some limits as to the parental magma from which the ring structures developed during the collapse phase of the original volcano, (cauldron subsidence).Taken this into consideration i.e., assuming a trachytic magma as a source material for the development of the syenitic outer and inner rings. Rare earth elements modeling calculations have been successfully used for the derivation of granitic rocks by partial melting and/or crystal fractionation from sources of intermediate composition.

A trachyandesite from the Afar Rift, Ethiopia, ( Barberi, et al., 1975), has been chosen to represent the REE composition of the parent magma, both belonging to the Red Sea Rift system. The modal mineralogy of the trachyandesite comprises 40% plagioclase, 40% K- feldspar, 15% hornblende, 3% biotite and 3% quartz.

Using the Newpet program and fractional crystallization model ;where the crystallizing phases comprise 90% plagioclase and 10% hornblende. It was found that the REE composition of the outer ring structure was achieved at 49% fractional crystallization whereas that the inner ring structure was achieved at 53% crystal fractionation. The calculated models along with the range of the actual REE data of the outer and inner rings are shown in Figs. (36 and 37 ).The REE pattern of the source trachyandesite is shown for comparison. The calculated REE composition of residual solid is calculated and its pattern is shown in Fig. (37).Such REE pattern is consistent with that of an alkaline basalt. This is consistent with the presence of a central gabbroic stock in El Kahfa ring complex.

**Geochemistry of U and Th.**

Uranium and thorium contents were determined chemically in 14 samples The obtained results of the uranium and thorium analyses as well as Th/U ratios are shown in Table (3). From this table, the uranium content of Gabal El Kahafa ring complex ranges from 1.9 to 10.5 ppm with an average 5.14 ppm and thorium content ranging from 5.45 to 32.7 ppm with an average of 17.5 ppm,. Which are consistent with the average U and Th of the granitic rocks of Clark et al.(1966), and also compatible in the range of the acidic intrusive rocks of Adams et al.(1959) and the silicic intrusive rocks of Rogers and Adams(1967).

The geochemical behaviour of U and Th in the studied areas as indicating by the U-Th variation diagram which shows for the studied rocks

indicate strong positive relations between the two elements due to magmatic origin as shown in (Fig. 38).

Fig.( 39) shows that the variation of Th/U ratios versus U in the studied rocks . It is clear from the figure that the decrease of Th/U ratio is accompanied with enrichment in U. Also, the behavior of U and Th with respect to Rb is shown in Figs. (40&41), where there is a good positive correlation between U and Rb which seems that U follows Rb through magmatic fractionation. Also, the behavior of Th respect to Rb is shown in Fig. (41), shows positive correlation between the two elements. This proves a close link between Rb, Th and U in the evolution of magmatic series whether this evolution follows magmatic. From the above it is clear that the U and Th contents are controlled by the presence of some accessory minerals (zircon, allanite, apatite and iron oxides) whereas iron oxide and hydroxides are know to adsorb U from circulating fluids.

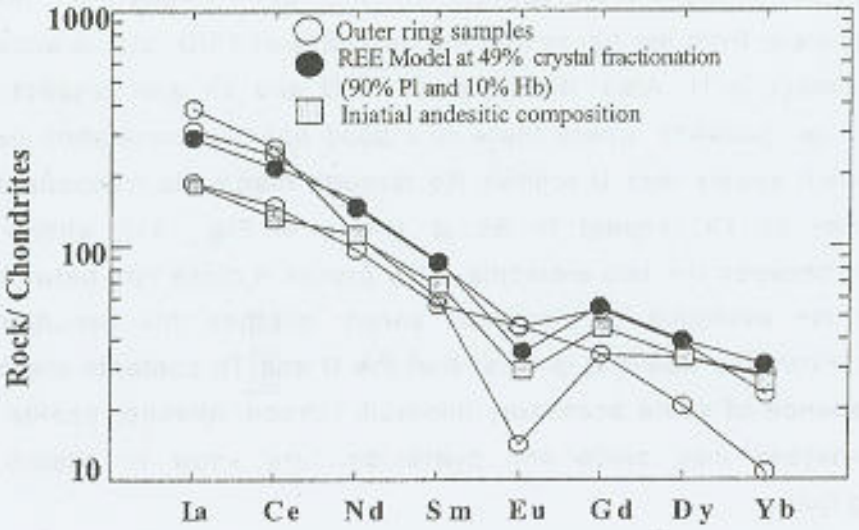


(Fig. 36 ) Model REE pattern for the outer ring samples

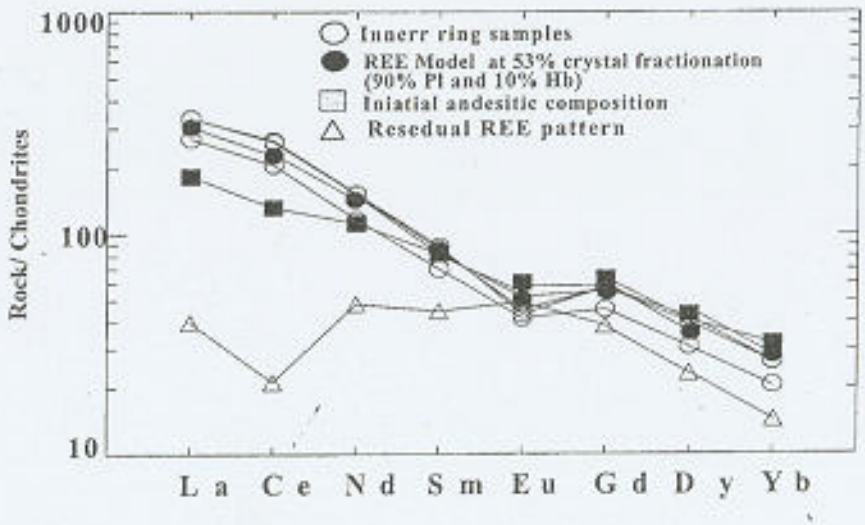


(Fig. 37) Model REE pattern for the inner ring samples

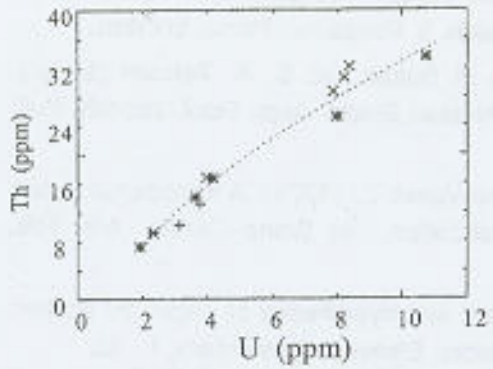


Fig. (38): Th-U variation diagram.

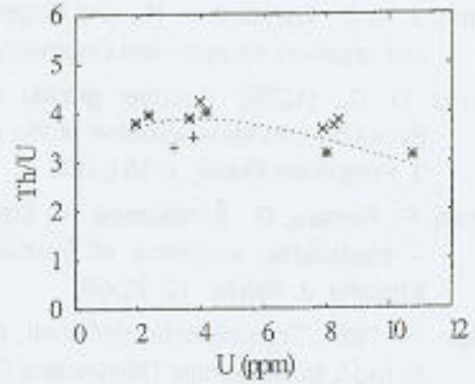


Fig. (39): Th/U -U variation diagram.

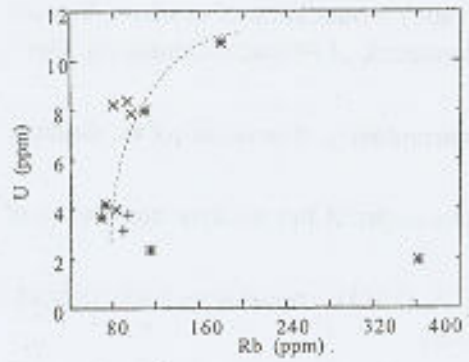


Fig. (40): U-Rb variation diagram.

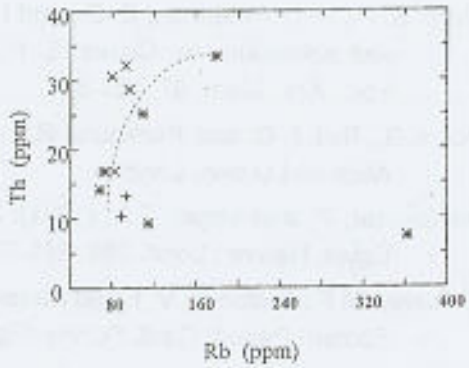


Fig. (41): Th-Rb variation diagram.

## References


Adams, J. A. S., Osmond, Y. K., and Rogers, J. J. W., (1959): The geochemistry of thorium and uranium, Physics and Chemistry of the Earth, 3, Pergamon Press, London.

Almond, D. C., (1979): Younger granite complexs of Sudan. In: S. A. Tahoun (Editor), Evolution and Mineralization of the Arabian- Nubian Shield. Appl. Geol. Jaddah, Bull. 3, Pergamon Press, 1: 151-164.

Barberi, F., Ferrara, G., Santacroce, R., Treuil, M. and Vavet, J., (1975): A transitional basalt – pantellerite sequence of fractional crystallization, the Boina Centre, Afar Rift, Ethiopia. J. Petrol., 16, 22-56.

Barker, F., 1979: Trondhjemite: definition, environment and hypotheses of origin. In: Barker, F. (ed.), trondhjemite, Dacites and Related Rocks. Elsevier, Amsterdam, 1– 12.

Bateman P. C. and Chappell, B. W. (1979): Crystallization, fractionation and solidification of the Toulumne intrusive series Yosemite National Park, California. Bull. Geol. Soc. Am., 90, 465-482.

Bonin, (1986): Ring Complex Granitoid and Anorogenic Magmatism, North Oxford Academic: A Division of Kogan, 189p.

Clark, S. P., Jr. , Peterman, Z. E., and Heier, K. S., (1966): Abundance of uranium, thorium and potassium, In: Clarke, S. P. Jr., (ed.), Handbook of Physical Constants, Geol. Soc. Am. Mem. 97, 521-541.

Cox K.G., Bell J. D. and Pankhurst RJ.,(1979): The interpretation of igneous rocks. George, Allen and Unwin, London.

De Gruyter, P. and Vogel, T.A. (1981): A model for the origin of the alkaline complexes of Egypt. Nature , Lond. 291, 571-574.

El Ramly, M.F., Budanov, V. I. and Abdel Aziz Hussein, A. (1971): The alkaline rocks of south Eastern Desert: Geol. Survey (Egypt), paper no.53.

El Ramly, M.F., Budanov, V. I., Armanious, I. K. and Dereniuk, N. E. (1969): The ring complexs of Gebel El Kahfa, Gebel Nigrub El Fogani, Gebel El Naga: Geol. Survey (Egypt), papar no.52.

Gast, P. W., (1965):Terrestial ratio of potassium to rubdium and the compostion of the Earths mantle, Science,147, 858-860.

Girdler, R. W. (1970) : A review of Red Sea heat flow. Phil.Trans. Roy. Soc. London 267(A): 191-203.

Goldschmidt, V. M., (1954): Geochemistry, Oxford Univ. Press, Oxford, England.

Greenberg, J.K. (1981): Characteristics and origin of Egyptian younger granites. Geol. Soc. America Bull., part I, 92, 224-256.

Griffin, W. L., and Murthy, V. R., (1969): Distribution of K, Rb Sr and Ba in some minerals relevant to basalt genesis. Geochem. Cosmochim. Acta, 33., 1389-1414.

Hashad, A. H. and El Reedy, M.W.M.(1979): Geochronology of the anorogenic alkalic rocks. South Eastern Desert, Egypt. Ann. Geol. Surv. Egypt. 9, 81-101.

Heier, K. S., (1973): Geochemistry of granulite facies rocks and problems of their origin. Phil. Trans Roy. Soc. Lond.., A 273, 429-442.

Irvine, I. N. and Baragar, W. R. A., (1971): A guide to the chemical classification of common volcanic rocks, Can. Jour. Earth Sci., 81, 523-548.

IUGS (1989): A classification of igneous rocks and glossary of terms. Le Maitre (ed.), Blackwell, Oxford. 193pp.

James, R. S. and Hamilton, D. L. (1969): Phase relations in the system $NaAlSi_3O_8$-$KAlSi_3O_8$-$CaAl2SiO_8$-$SiO_2$ at 1 kilobar water vapour pressure. Contrib. Mineral. Petrol., 21, 111-141.

Le Maitre, R. W. (1989): A classification of igneous rocks and glossary of terms recommendation of the international Union of Geological Sciences Subcommission on the Systematics of Igneous Rocks. Blackwell Scientific Publications, London; 193p.

Maniar, P. D., and Piccoli, P. M., (1989): Tectonic discrimination of granitoids, Geol. Soc. Am. Bull., 101, 635-643.

Mason, B., 1966: Principles of Geochemistry, 3rd Ed., John Wiley and Sons Inc., New York, 329.

Meneisy, M., (1990): Volcanicity. In: Said, R. (Ed.), The Geology of Egypt, A. A. Balkema, Rotterdam. 157-174.

Middlemost. E. A. K., (1985): Magmas and magmatic rocks. Longman, London.

O'Connor, J. T., (1965): A classification of quartz-rich igneous rocks based on feldspar ratios, U.S. Geol. Surv., Prof. Pap. 525B, B79-B84.

Pearce, J. A., Harris, N. B. W. and Tindle, A. G. (1984): Trace element discrimination diagrams for the tectonic interpretation of granitic rocks. Jour. Petrol., 25, 956-983.

Petro, W. L., Vogel, T. A. and Wilband, J. T. (1979): Major element geochemistry of plutoniv rock suites from compressional and extensional plate boundaries: Chem. Geol., V.26, P. 217-235.

Rogers, J. J. W., and Adams, J. A. S., (1969): Uranium and throium, In: (ed. K.H. Wedepohl) Handbook of Geochemistry, II-3, 92-B-1 to 92-0-8 and 90-B-1 to 90-0-5 In. Springer Verlag.

Serencsits, C.Mc.C, Faul, H., Roland K.A.,.Hussein A.A., and Lutz, T.M (1981): Alkaline ring complexes in Egypt: their ages and relationship in time. J. Geophys. Res. 86:3009-3013.

Serencsits, C.Mc.C, Faul, H., Roland K.A., El Ramly, M. F. Hussein A.A., and Lutz, T.M. (1979): Alkaline ring complexes in Egypt: their ages and relationship to tectonic development of the Red Sea. Ann. Geol. Surv. Egypt 9:102-116.

Stoeser, D. B. and Elliott, J. E. (1980): Post-orogenic peralkaline and calc-alkaline granites and associated mineralization of the Arabian Shield, Kingdom of Saudi Arabia. In: P. G. Cooray and S. A. Tahoun (Editors), Evolution and Mineralization of the Arabian-Nubian Shield. Appl. Geol. Jaddah, Bull. 3, Pergamon Press, 4: 1-23.

Streckeisen, A. L. (1976): Classification of the common igneous rocks by means of their chemical compositions. A provisional Attempt. N. Jb. Min. Jour.,1-15.

Stern, R. J. and Hedge C. E., (1985): Geochronology and isotopic constraints on late Precambrian crustal evolution in the (ED), Egypt. Am. J. Sci., v. 285,P97-127.

Sun, S. S.(1980): Lead isotopic study of young volcanic rocks from mid-ocean ridges, ocean islands and island arcs. PHIL Trans R. Soc. Lond. A279-45.

Taylor, S. R. (1965): The application of trace element data to problems in petrology. In: Physical and Chemistry of the Earth (ed.); Ahrens, L. H., Press. F., Runcor, S. K. and Urey, H. C., 133-213

Taylor, S. R., McLennan S. M. (1985): The continental crust: its composition and evolution. Blackwell, Oxford, 312pp.

Tuttle, O. F. and Bowen, N. L., (1958): Origin of granite in the light of experimental studies in the system $NaAlSi_3O_8$-$KAlSi_3O_8$-$SiO_2$-$H_2O$. Geol. Soc. Am. Mem., 74, 153p.

Vail, j. R. (1989): Ring complexes and related rocks in Afrrica,.J. Afr. Earth Sci. 8,19-40. Vail, j. R. (1985): Alkaline ring complexes in Sudan.J. Afr. Earth Sci. 3:51-59.

Vail, j. R. (1985): Alkaline ring complexes in Sudan.J. Afr. Earth Sci. 3:51-59.

Vail, j. R. (1984): Distribution and tectonic setting of post-kinematic igneous complexes in the Red Sea hills of Sudan and Arabian-Nubian Shield. Bull. Fac. Earth. Sci., King Abualaziz Univ., Jeddah, 6,259-270.

Wilson, M. (1998) : Igneous Petrogenesis : Unwin Hyman, London, 466p.

Winkler, H. G. F., Boese, M., and Macropoulos, T., (1975): Low temperature granitic melts. N. Jb. Mineral., 6, 245-262.

Delta J. Sci.(Geo.) 32: 1 -31(2008)

# نشأة المعقدة الحلقية لجبل الكهفة- الصحراء الشرقية- مصر

وفقي السيد عبدالهادي النجار

هيئة المواد النووية – ص. ب . 520 المعادي- القاهرة- مصر.

تقع معقدة جبل الكهفة في الصحراء الشرقية لجمهورية مصر العربية وهي من النوع الغير كامل ومفتوحة في اتجاه الجنوب وتتداخل هذه المعقدة في صخور الدايوريت والبورفيريت وتتكون في الجزء الخارجي من صخور السيانيت القلوي وفي الجزء الداخلي من صخور السيانيت القلوي وصخور السيانيت النفيليني مع وجود صخور الجابرو وبعض القواطع بالجزء الأوسط ثم تحركت هذه المعقدة خلال مرحلتين رئيسيتين من النشاط وهما المرحلة الأولى وتشمل الجزء الخارجي (outer ring) المتمثل بالجزء ذو اللون الأبيض والمرحلة الثانية وتشمل الجزء الداخلي ( inner ring) المتمثل بالجزء ذو اللون الأحمر .وقد أوضحت الدراسة الجيوكيميائية أن صخور السيانيت تكونت من ماجما قلوية وافرة الألومنيوم في بيئة داخل الألواح التكتونية على أعماق ما بين ( 9 -21 )كم في درجات حرارة أكبر من 840° م ومن دراسة العناصر الأرضية النادرة يتضح أن تركيزها يزيد من الحلقة الخارجية الى الحلقة الداخلية ويبين أن الماجما تدافعت على ثلاث دفعاتوأن الحلقة الخارجية تكونت من تمايز بلوري بنسبة49 % وأن الحلقة الخارجية تكونت من تمايز بلوري بنسبة 53%.تعزى اشعاعية هذه الصخور الى تواجد عنصري اليورانيوم والثوريوم المرتبطين بالعمليات المجمانية وتواجدات بعض المعادن الاضافية مثل الزركون والأباتيت وأكاسيد الحديد.